

The Au(111)/Electrolyte Interface: A Tunnel-Spectroscopic and DFT Investigation**

Felice C. Simeone, Dieter M. Kolb, Sudha Venkatachalam, and Timo Jacob*

Distance tunneling spectroscopy in combination with density functional theory calculations has been employed to derive a detailed model of the electric double layer for Au(111) in 0.1M H₂SO₄ at $E \geq +0.8$ V vs. SCE. At such positive potentials, the specifically adsorbed sulfate ions on gold form the well-known ($\sqrt{3} \times \sqrt{7}$)R19.1° superstructure.^[1–6] Herein, we present for the first time experimental and theoretical evidence for the double-layer structure normal to the surface. In addition, the DFT calculations also allowed the determination of the absolute width of the tunnel gap.

The structure of the electric double layer at metal–solution interfaces, which can be considered the site for electrochemical reactions, is still an area of intense research.^[7,8] This is particularly true for the solution side of the double layer, the knowledge of which stems mostly from thermodynamic data.^[9] Besides X-ray diffraction and infrared absorption methods,^[1,10,11] scanning tunneling spectroscopy is capable of yielding valuable structure information normal to the surface, which otherwise is difficult to obtain.^[12–14] However, while the imaging of electrode surfaces with STM in an electrochemical cell under operating conditions (under potential control) is by now a well-established technique,^[15,16] tunneling spectroscopy of the electrochemical interface is still in its infant stage.^[12–14,17,18] This situation is not the least caused by experimental problems, arising from the rather limited potential window set by the decomposition potential of aqueous solutions and by the fact that the tunnel voltage between tip and sample not only governs the tunneling process, but also the electrochemistry at the tip and sample surface. This problem is particularly relevant for the so-called current–voltage spectroscopy,^[19] in which the potential of the sample or tip (or of both) is varied. Such problems are less severe for distance tunneling spectroscopy, in which the tunneling current I_T is recorded as a function of tip distance s ,

and the potentials of the sample and tip (and hence tunnel voltage) are held constant.

At electrified interfaces the tunnel current decay with increasing distance from the surface is not strictly exponential, but shows a more complicated dependence on the distance and on the electrode potential.^[12–14,17,18,20] For example, Schindler et al. have shown that the effective barrier height (EBH) [Eq. (1)] varies with distance from a gold electrode surface in an “oscillatory” way, which has been interpreted as being due to the structure of interfacial water.^[13]

$$\phi_T = \frac{\hbar^2}{8m} \left(\frac{\partial \ln I_T}{\partial s} \right)^2 \quad (1)$$

However, a direct correlation between the observed structure in $\phi_T(s)$ and the spatial distribution of double-layer constituents (ions and water) normal to the surface without theoretical support is almost impossible. On the other hand, such information may be considered the “missing link” in double-layer studies: Whereas there is a wealth of data on the lateral distribution of anions on single-crystal noble-metal electrodes, information on charge and ion or solvent distribution normal to the surface is scarce.

Figure 1 shows the tunnel current as a function of distance for Au(111) in 0.1M H₂SO₄ at +0.8 V vs. SCE, together with the corresponding curve for the EBH as determined by Equation (1). The tip potential was kept at +0.275 V vs. SCE, that is, the tunnel voltage was 525 mV. The smallest, experimentally achieved distance between tip and sample ($s' = 0$) is for $I_T = 800$ nA, the maximum tunnel current that can be handled by our equipment. This distance, however, is by no means identical with the tunnel gap s , the knowledge of which is required for a meaningful discussion of the experimental data.

By definition, $s = 0$ at the point contact of the tip and substrate,^[21] for which the quantum contact resistance is $G^{-1} = 12.9$ k Ω . Because tip–substrate contacts usually deviate from ideal quantum point contacts in reality, Lang introduced an effective contact resistance $R = Ah/e^2$, where A is a material-dependent constant greater than 1.^[22] By choosing $A = 2.7$ ($R = 35$ k Ω), he could satisfactorily reproduce experimental results obtained under UHV conditions.^[23] However, for metal–solution interfaces even $R = 35$ k Ω would lead to unrealistically large s values, indicating that tunnel currents in general are lower in that case. This observation might be rationalized by a pronounced change in the pre-exponential factor owing to the strong chemical interaction between adlayer and metal surface. We therefore tried to determine

[*] Dr. S. Venkatachalam, Dr. T. Jacob
Theory Department
Fritz-Haber-Institut der Max-Planck-Gesellschaft
Faradayweg 4–6, 14195 Berlin (Germany)
Fax: (+49) 30-8413-4701
E-mail: jacob@fhi-berlin.mpg.de
F. C. Simeone, Prof. Dr. D. M. Kolb
Institute of Electrochemistry
University of Ulm
89069 Ulm (Germany)
E-mail: dieter.kolb@uni-ulm.de
Homepage: <http://www.uni-ulm.de/echem>

[**] Support by the Fonds der Chemischen Industrie (FCI), the Deutsche Forschungsgemeinschaft, and the Alexander von Humboldt Foundation (AvH) is gratefully acknowledged.

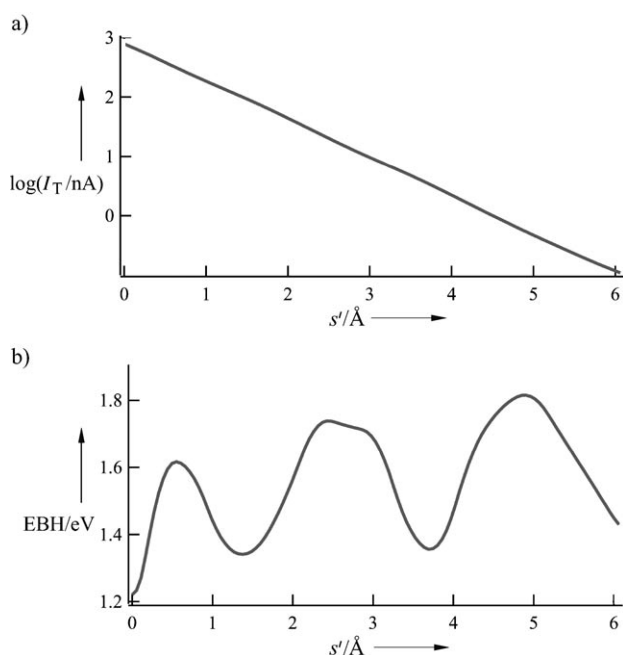


Figure 1. Tunnel current (a) and effective barrier height (b) versus distance for Au(111) in 0.1 M H_2SO_4 at +0.8 V vs. SCE; $s'=0$ is the smallest experimentally achieved distance between the tip and sample. Note that $\log(I_T)$ vs. s' is not strictly linear.

our setpoint $s=0$ by adjusting the experimentally derived EBH data to the calculated distances.

To obtain an atomistic picture of the structure at the interface between the electrolyte and the Au(111) electrode, we performed DFT calculations on the $(\sqrt{3} \times \sqrt{7})\text{R}19.1^\circ$ sulfate superstructure. Although the periodicity of the adlayer is well-studied,^[1,4,24] there is still no clear conclusion on the nature of the coadsorbates, which have also been observed by in situ STM (Figure 2b). Therefore, in our DFT studies we have considered the coadsorption of water and hydronium ions in different combinations and structures. As one might expect for the pH value used in our experiments, we find that the calculation with coadsorption of a single hydronium ion per unit cell showed the best agreement with our previous in situ STM measurements^[24] and with the distance tunneling data presented here. Therefore, under these conditions we can rule out the specific adsorption of bisulfate as well as water at the electrode surface. A top view of this system together with the corresponding STM measurement is shown in Figure 2, while the side view of a single unit cell together with the analysis is shown in Figure 3.

In this system the lower three oxygen atoms of the sulfate ion, which bind to the surface, are on average 2.38 Å above the surface, forming each a single covalent bond to the corresponding Au atom below. In addition, each of these O atoms binds to the central S atom with $d(\text{S}-\text{O}) \approx 1.55 \text{ Å}$. While two of these O atoms show an equivalent behavior, the oxygen atom, which is also hydrogen-bonded ($d(\text{O}-\text{H}) = 1.74 \text{ Å}$) to two adjacent hydronium ions, forms somewhat weaker S–O and Au–O bonds, which leads to a slight increase of both bond lengths. While the sulfate ion mainly orients with respect to the underlying substrate, the position of the

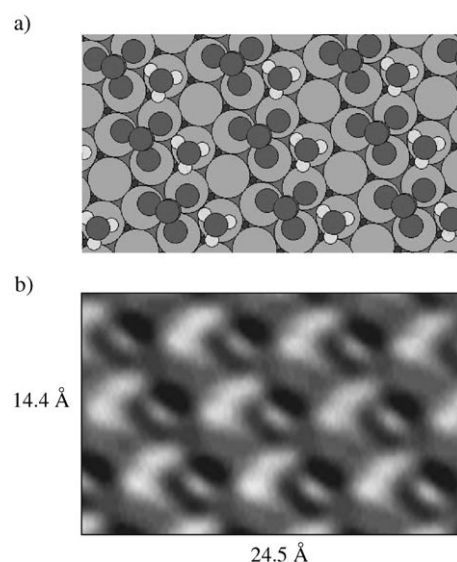


Figure 2. a) Geometry-optimized structure of $(\sqrt{3} \times \sqrt{7})$ sulfate coadsorbed with hydronium ions (Au: large circles; the S atoms are located under the central O atoms) and b) the corresponding STM image at +0.8 V vs. SCE.

hydronium ion is determined by its ability to form hydrogen bonds, for which we find a preference of the O atom to be above the plane formed by the three H atoms (see Figure 3).

To relate our distance tunneling spectroscopy measurements to an absolute vertical position with respect to the surface plane we adjusted the first peak in the curve to the plane formed by the three lower oxygen atoms of the sulfate ion. This procedure is justified by the fact that the STM-measured EBH should reflect the distribution of negative charge density, for which the analysis of our DFT calculations showed an accumulation at the distance to the surface of these oxygen atoms (see Figure 3). On this distance scale the first minimum is $3.2\text{--}3.3 \text{ Å}$ above the surface plane, which interestingly coincides with the vertical position of the O atom of the hydronium ion. This result clearly shows that correlating the position of the current peaks from the distance tunneling spectroscopy with the oxygen atoms in the system is not sufficient. However, there is a correlation with the charge density distribution, which at the surface distance of the first minimum shows a pronounced accumulation of positive charge density (electron depletion) coming from the sulfur atom and the hydrogen atoms (of the hydronium ion). Moving the STM tip further away from the surface, we find two peaks close to each other at 4.3 and 4.8 Å . These two peaks find their direct correspondence in the calculated charge density distribution, which identifies the first peak at 4.3 Å as negative charge accumulated slightly above the oxygen atom of the hydronium ion (occupying a p orbital) and the second peak as negative charge being located at the topmost O atom of the sulfate ion. Although our DFT calculations (only) consider specific adsorption, the minimum in the STM curve at around 5.5 Å and the following maximum at around 6.9 Å most probably reflect the next water layer, which hydrates the adsorbates on the electrode, and the outer Helmholtz plane, respectively.

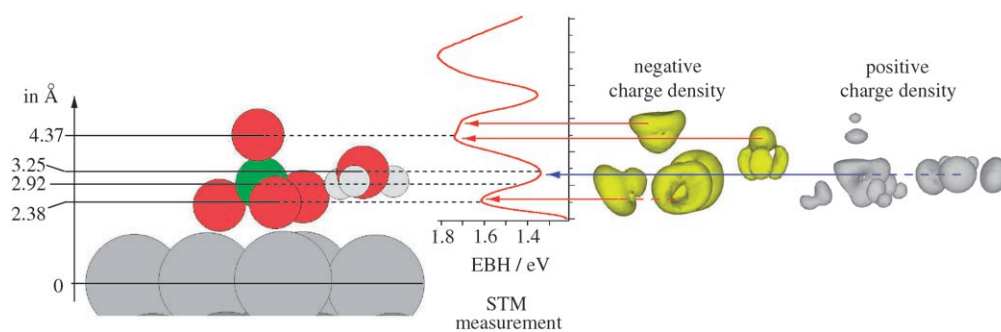


Figure 3. Comparison of the DFT-calculated structure with the STM measurement. Left: Side view of a single ($\sqrt{3} \times \sqrt{7}$) unit cell as shown in Figure 2, including the vertical distances of the different atoms to the first surface layer; middle: STM measurement, whereby the vertical position has been adjusted such that the lowest peak meets the lower oxygen atoms of the sulfate ion; right: distribution of negative and positive charge density obtained from the DFT calculations. The vertical positions correspond to the parent hard-sphere model shown in the sphere model (left).

In summary, this work for the first time reveals an atomistic view of the gold–electrolyte interface, demonstrating how the combination of experimental measurements and theoretical calculations can provide new insights into systems as complex as electrochemical interfaces. Only by this combination of theory and experiment we were able to provide an absolute distance scale for the distance tunneling measurements, without the need to make additional assumptions on the basis of the STM tip resistance at point contact.

Experimental Section

The Au(111) single crystal (Mateck, Jülich, Germany), about 10 mm in diameter and 2 mm thick, was flame-annealed for about 6 min at red heat before each measurement.^[25] The electrolyte, usually 0.1M H_2SO_4 , was made from Merck (Suprapure) and Milli-Q water. A Pt wire served as reference electrode, but all potentials are quoted with respect to the saturated calomel electrode (SCE). The microscope for the STM measurements was placed in a sealed plastic box, where an argon atmosphere was maintained. Any presence of oxygen in the solution was detected by cyclic voltammetry. Several cyclic voltammograms of the tip and the sample were executed before each experiment to electrochemically stabilize the system.

The tunnel current–distance $I_T(s)$ curves were recorded with a scanning tunneling microscope (DI, Nanoscope E III, Santa Barbara) by first setting 800 nA as the current set point to fix the distance. This was the maximum value that could be handled by our modified tip preamplifier. Then, the feedback loop of the STM was switched off, and $I_T(s)$ traces were recorded while the tip was retracted from the surface and approached again at a rate of 2.3–6 nm s^{-1} , a velocity that minimizes thermal drift effects from the STM scanner. Then the feedback was briefly reactivated to check and eventually correct the position on the surface before two new curves (forward and backward) were recorded. For $E = +0.8 \text{ V}$ vs. SCE, the measurements were repeated at different places on the surface. The curves were considered valid only when the tip gave good atomic resolution before and after the $I_T(s)$ measurements, and when the forward and backward currents were, within given limits, identical. The z calibration of the STM scanner was checked before and after each session.

The curve shown in Figure 1a is an average of 500 curves recorded with different tips and on different days. To calculate the EBH (Figure 1b) directly from the experimental data by using Equation (1), uniformly spaced $I_T(s)$ data points were produced with a cubic spline algorithm,^[26] which allows also for a filtering of any

noise arising from the electronics, from faradaic currents at the tip, and from the stepped movement of the piezo element.

To complement the experimental studies we used SeqQuest,^[27] a periodic DFT program with localized basis sets represented by a linear combination of Gaussian functions, together with the PBE^[28] GGA exchange–correlation functional. The core electrons of each Au atom were replaced by a standard (nonlocal) norm-conserving pseudopotential,^[29] leaving the 5d and 6s electrons in the valence space and invoking a nonlinear core correction.^[30]

The basis sets were optimized with “double zeta plus polarization” contracted Gaussian functions.

All calculations were performed on a six-layer slab, where the lowest two layers were fixed to the calculated bulk crystal structure ($a_0 = 4.152 \text{ \AA}$), while the remaining four surface layers and the adsorbates (modeled as neutral molecules) were allowed to fully optimize their geometry (to less than 0.01 eV/Å). Integrations in the reciprocal space were performed with a converged Brillouin zone sampling of $8 \times 5 \times k$ points for the ($\sqrt{3} \times \sqrt{7}$) unit cell.

Received: June 28, 2007

Revised: August 19, 2007

Published online: October 12, 2007

Keywords: density functional calculations · distance tunneling microscopy · electrochemistry · interfaces · sulfate

- [1] Z. Shi, J. Lipkowski, M. Gamboa, P. Zelenay, A. Wieckowski, *J. Electroanal. Chem.* **1994**, 366, 317.
- [2] G. J. Edens, X. Gao, M. J. Weaver, *J. Electroanal. Chem.* **1994**, 375, 357.
- [3] I. R. de Moraes, F. C. Nart, *J. Electroanal. Chem.* **1999**, 461, 110.
- [4] A. Cuesta, M. Kleinert, D. M. Kolb, *Phys. Chem. Chem. Phys.* **2000**, 2, 5684.
- [5] T. Wandlowski, K. Ataka, S. Pronkin, D. Dising, *Electrochim. Acta* **2004**, 49, 1233.
- [6] K. Sato, S. Yoshimoto, J. Inukai, K. Itaya, *Electrochem. Commun.* **2006**, 8, 725.
- [7] A. Guidelli, W. Schmickler, *Electrochim. Acta* **2000**, 45, 2317.
- [8] E. Wernersson, R. Kjellander, *J. Chem. Phys.* **2006**, 125, 154702.
- [9] R. Parsons in *Comprehensive Treatise of Electrochemistry, Vol. 1* (Eds.: J. Bockris, B. Conway, E. Yeager), New York, **1980**, p. 1.
- [10] K. Ataka, M. Osawa, *Langmuir* **1998**, 14, 951.
- [11] M. Ito, M. Yamazaki, *Phys. Chem. Chem. Phys.* **2006**, 8, 3623.
- [12] G. Nagy, *Electrochim. Acta* **1995**, 40, 1385.
- [13] M. Hugelmann, W. Schindler, *J. Electrochem. Soc.* **2004**, 151, E97.
- [14] G. Nagy, T. Wandlowski, *Langmuir* **2003**, 19, 10271.
- [15] K. Itaya, *Prog. Surf. Sci.* **1998**, 58, 121.
- [16] D. M. Kolb, *Electrochim. Acta* **2000**, 45, 2387.
- [17] R. Hiesgen, D. Eberhardt, D. Meissner, *Surf. Sci.* **2005**, 597, 80.
- [18] J. Halbritter, G. Repphun, S. Vinzelberg, G. Staikov, W. J. Lorenz, *Electrochim. Acta* **1995**, 40, 1385.

- [19] P. Hugelmann, W. Schindler, *J. Phys. Chem. B* **2005**, *109*, 6262.
[20] D. M. Kolb, F. C. Simeone, *Electrochim. Acta* **2005**, *50*, 2989.
[21] H. Ohnishi, Y. Kondo, K. Takayanagy, *Nature* **1998**, *395*, 780.
[22] N. D. Lang, *Phys. Rev. B* **1987**, *36*, 8173.
[23] N. D. Lang, *Phys. Rev. B* **1988**, *37*, 10395.
[24] O. M. Magnussen, J. Hageböck, J. Hotlos, R. J. Behm, *Faraday Discuss.* **1992**, *94*, 329.
[25] L. A. Kibler, *Preparation and characterization of noble metal single crystal electrodes*, <http://www.uni-ulm.de/echem/ekat/downloadpage.html>.
[26] C. H. Reinsch, *Numer. Math.* **1967**, *10*, 177.
[27] C. Verdozzi, P. A. Schultz, R. Wu, A. H. Edwards, N. Kioussis, *Phys. Rev. B* **2002**, *66*, 125408.
[28] J. P. Perdew, K. Burke, M. Ernzerhof, *Phys. Rev. Lett.* **1996**, *77*, 3865.
[29] D. R. Hamann, *Phys. Rev. B* **1989**, *40*, 2980.
[30] S. G. Louie, S. Froyen, M. L. Cohen, *Phys. Rev. B* **1982**, *26*, 1738.
-